

Residual Tensor Train: a Flexible and Efficient Approach for Learning Multiple Multilinear Correlations

Yiwei Chen, Yu Pan, *Senior Member, IEEE*, Daoyi Dong, *Senior Member, IEEE*

arXiv:2108.08659v1 [cs.LG] 19 Aug 2021

Abstract—Tensor Train (TT) approach has been successfully applied in the modelling of the multilinear interaction of features. Nevertheless, the existing models lack flexibility and generalizability, as they only model a single type of high-order correlation. In practice, multiple multilinear correlations may exist within the features. In this paper, we present a novel Residual Tensor Train (ResTT) which integrates the merits of TT and residual structure to capture the multilinear feature correlations, from low to higher orders, within the same model. In particular, we prove that the fully-connected layer in neural networks and the Volterra series can be taken as special cases of ResTT. Furthermore, we derive the rule for weight initialization that stabilizes the training of ResTT based on a mean-field analysis. We prove that such a rule is much more relaxed than that of TT, which means ResTT can easily address the vanishing and exploding gradient problem that exists in the current TT models. Numerical experiments demonstrate that ResTT outperforms the state-of-the-art tensor network approaches, and is competitive with the benchmark deep learning models on MNIST and Fashion-MNIST datasets.

Index Terms—multilinear correlation, tensor train, machine learning, residual connection

I. INTRODUCTION

A booming progress in computational hardware has led to a continuing and rapid evolution of machine learning. Linear approaches, such as linear regression model [1] and support vector machines [2], assume linear correlation between the features to solve classification and regression problems. However, due to the complexity of underlying patterns, a simple linear approach may underfit the data for a variety of applications [3]. In [4], a bilinear model has been utilized to solve two-factor tasks, such as separating the style and content of handwritten digits. Since then, low-order feature interactions, including bilinear and trilinear correlations, have been widely adopted to improve the capability of modelling the multilinearity hidden in data [5]–[8].

For high-order feature interactions, the dimensionality issue leads to expensive computational and memory cost. Tensor Train (TT) [9]–[11], which is considered as an efficient way to reduce the parameters for high-order tensors, has inspired a novel machine learning approach to model multilinear feature

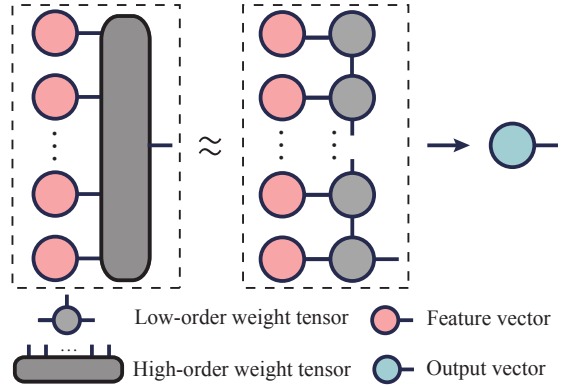


Fig. 1. The left figure is the tensor network representation of the input features contracting with the high-order weight tensor. In the middle figure, the high-order weight tensor is replaced by the one-dimensional TT. The contraction between the TT and input features generates an output vector.

interactions, and demonstrated superior performance in computer vision [12]–[14] and recommendation system tasks [15]. As shown in Fig. 1, the TT approach replaces a high-order weight tensor by a one-dimensional chain of low-order tensors that significantly reduces the number of trainable parameters. However, for an N -order input which is the tensor product of N features, the existing TT approaches only capture its N -order multilinear correlation. In practice, linear, bilinear and higher-order correlations may exist simultaneously between the features, and thus a more generalized model needs to be built to cover these scenarios and achieve improved performance.

In this paper, we propose a Residual TT (ResTT) which is capable of modelling multiple multilinear feature interactions within the same network. The main innovation of ResTT is incorporating skip connections [16] into the present TT. By designing the network topology of skip connections, the ResTT can flexibly model diverse types of feature interactions. The main advantages of ResTT and contributions of this paper are summarized as follows:

- ResTT is able to learn multiple multilinear feature correlations in a data-driven way. Besides, ResTT can flexibly model a diverse set of feature interactions by simply modifying the skip connections. In particular, by designing the network topology of skip connections, ResTT can be reduced to the fully-connected layer in neural networks [17] and Volterra series [18]. In other words, the fully-

Y. Chen is with the Institute of Cyber-Systems and Control, Zhejiang University, Hangzhou, 310027, China. (email: ewell@zju.edu.cn).

Y. Pan is with the Institute of Cyber-Systems and Control, College of Control Science and Engineering, Zhejiang University, Hangzhou, 310027, China. (email: ypan@zju.edu.cn).

D. Dong is with the School of Engineering and Information Technology, University of New South Wales, Canberra, ACT 2600, Australia. (email: daoyidong@gmail.com).

connected layer and Volterra series can be looked as special cases of ResTT.

- ResTT is immune to the gradient vanishing and exploding problem under much more relaxed condition than that of traditional TT. Due to the large number of contractions, the training of TT may be unstable and the training process will freeze unexpectedly [15]. In this paper, we have extended the mean-field analysis [19] to TT models for deriving the rules of initialization that stabilize the training process. It is found that the variance of input features will disturb the training of TT, and a strict initial condition has to be satisfied to ensure its stability. In contrast, the stability condition for ResTT is significantly relaxed, and no strict restrictions are imposed on the statistics of the input features.
- Extensive experiments are conducted on the synthetic dataset, MNIST [20] and Fashion-MNIST [21] datasets. Experimental results demonstrate that ResTT consistently outperforms the state-of-the-art tensor network models and achieves competitive advantage over the benchmark deep learning models. ResTT also demonstrates better performance than the multi-task learning approaches [22] for limited data. In particular, the convergence of ResTT is faster and more stable than other tensor network models.

The remainder of this paper is organized as follows. Sec. II provides a brief introduction to the background and related works. In Sec. III, we introduce ResTT in detail. Sec. IV presents the mean-field analysis for TT and ResTT. Sec. V presents the experimental results on the synthetic and real datasets. Finally, the conclusion is drawn in Sec. VI.

II. PRELIMINARIES

In this section, we first introduce the notation and definitions used in this paper and then we review the TT approach for supervised learning tasks [12]. Lastly, the related works are discussed.

A. Notation and definition

Definition 1 (Tensor): Tensor, also known as multidimensional or N -mode array, is a generalization of vector (one index) and matrix (two indices) to an arbitrary number of indices. In this paper, we denote tensors by calligraphic capitals. An N -order tensor is denoted by $\mathcal{A} \in \mathbb{R}^{I_1 \times I_2 \times \dots \times I_N}$, in which I_n ($1 \leq n \leq N, n \in \mathbb{N}^+$) is the dimension of the n -th index. The element of \mathcal{A} is denoted by $a_{i_1 i_2 \dots i_n}$ ($1 \leq i_n \leq I_n, I_n \in \mathbb{N}^+$).

The diagrammatic notation for a tensor is drawn as a circle with edges, in which the circle represents the elements of the tensor and the edges represent its each individual index. For example, the graphics shown in Fig. 2 (a) represent vector (1-order tensor), matrix (2-order tensor), 3-order tensor and N -order tensor, respectively.

Definition 2 (Tensor Contraction): Tensor contraction is an operation that combines two or more tensors into a new one. In this paper, we denote tensor contraction by $C_{I_k}[\cdot]$, where I_k is the index to be contracted. For example, a matrix $\mathcal{M} =$

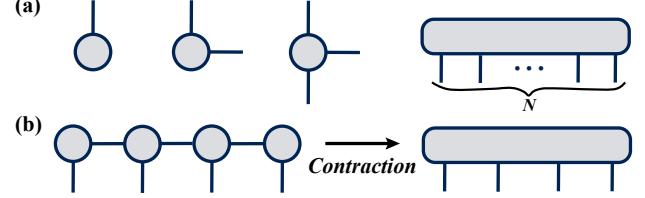


Fig. 2. Tensor network notation. (a) Graphical notations of tensors with different orders. (b) Contracting the four nodes in TT to obtain a 4-order tensor.

$\{m_{i_1 i_2}\} \in \mathbb{R}^{I_1 \times I_2}$ and a 3-order tensor $\mathcal{T} \in \mathbb{R}^{J_1 \times J_2 \times I_1}$ can be contracted along the index I_1 as

$$\mathcal{C} = C_{I_1}[\mathcal{M}, \mathcal{T}] \quad (1)$$

with $\mathcal{C} \in \mathbb{R}^{I_2 \times J_1 \times J_2}$ being the new 3-order tensor. The elements of \mathcal{C} are given by

$$c_{i_2 j_1 j_2} = \sum_{i_1} m_{i_1 i_2} t_{j_1 j_2 i_1}. \quad (2)$$

Note that the tensors to be contracted must have one or more compatible indices of the same dimension, such as the index I_1 in \mathcal{M} and \mathcal{T} .

In the graphical notation, a contraction is represented by a sharing edge, which indicates that the two tensor nodes are contracted along this particular index.

Definition 3 (Tensor Train): Tensor Train (TT) is a set of tensors to be contracted in a one-dimensional mode. Specifically, N tensors denoted by $\{\mathcal{W}^{(1)} \in \mathbb{R}^{I_1 \times V_1}, \mathcal{W}^{(2)} \in \mathbb{R}^{V_1 \times I_2 \times V_2}, \dots, \mathcal{W}^{(N)} \in \mathbb{R}^{V_{N-1} \times I_N}\}$ constitute a TT if contracted as

$$\mathcal{W} = C_{V_1, \dots, V_{N-1}}[\mathcal{W}^{(1)}, \mathcal{W}^{(2)}, \dots, \mathcal{W}^{(N)}], \quad (3)$$

where $\mathcal{W} \in \mathbb{R}^{I_1 \times \dots \times I_N}$ is the generated N -th tensor. V_1, V_2, \dots, V_{N-1} are called virtual bond dimensions.

The graphical representation of the contraction process of a 4-node TT is drawn in Fig. 2 (b). It is worth mentioning that the virtual bond dimensions could be used to control the total number of parameters.

Definition 4 (Feature interaction): In statistics, feature interaction [23] describes a situation in which the effect of one feature on the outcome depends on the state of other features. It is common to use products of features, also known as multilinear feature correlation, to represent different types of feature interaction. The number of features in the product term is defined as the order of interaction. For example, a bilinear model with an output y and two input features x_1 and x_2 is formulated as

$$y = c \cdot x_1 x_2, \quad (4)$$

where $c \cdot x_1 x_2$ describes the 2-order interaction between x_1 and x_2 .

B. Multilinear learning approaches

Linear methods are widely used in many applications [24]. However, optimal solutions may require considering higher-order feature interactions in complex problems. Early studies

of multilinear learning mainly focused on 2- and 3-order feature correlations. The work in [4] proposed an effective bilinear model to solve two-factor machine learning tasks. With the rapid development of computational hardware, low-order interactions have been widely adopted into machine learning models. The work in [25] utilized the bilinear correlation to construct a novel neural network layer, which provides a powerful way to describe relational information than the standard fully-connected layer. Combined with convolutional layers, such a layer has shown effectiveness in the question answering task [26]. Based on this idea, novel deep learning neural networks modelling bi- or tri-linear correlations have been proposed and demonstrated good performance in image classification [6], fine-grained image recognition [5], [8] and visual question answering [8]. The work in [27] proposed a bilinear model to exploit the task relatedness from feature interactions in multi-task learning.

Modelling high-order feature interactions is much more difficult than modelling low-order feature interactions due to the dimensionality issue. Recent multilinear learning frameworks, such as multilinear principal component analysis [28], usually employ dimensionality reduction techniques to simplify the original high-order tensor and cannot be trained by an end-to-end way. The TT method [15], [29] was proposed to extract the N -order dependencies among N input features on recommendation system tasks. After that, several approaches were proposed to use Matrix Product State (MPS) [12], [30], Tree Tensor Network (TTN) [31] and other types of low-dimensional tensor networks [32] on image classification and generation tasks. Besides, a tensor ring method [13] was proposed to capture high-order interaction in hyperspectral image. The work in [14] proposed a TT rounding procedure to determine the adaptive TT ranks instead of selecting ranks by experience. Multilinear correlation has also been incorporated into the compressive learning framework [33] which outperforms its vector-based counterpart in both inference performance and computational efficiency. However, as indicated by [15] and [31], the TT may fail to converge in training in case of a long chain, since hundreds of contractions are involved which will result in unbounded or vanishing outputs. Thus, specific normalization procedures must be embedded into the computation steps to keep the gradients in a reasonable range. More importantly, the current TT models lack generalizability and flexibility since only the N -order feature interaction is modelled, and none of them could comprehensively model multiple multilinear correlations.

C. Tensor Train Approach

Tensor train approach [12] provides an effective way to model high-order feature interactions. Given a set of feature vectors $\{\mathcal{X}^{(1)} \in \mathbb{R}^{I_1}, \mathcal{X}^{(2)} \in \mathbb{R}^{I_2}, \dots, \mathcal{X}^{(N)} \in \mathbb{R}^{I_N}\}$, the generalized network model is defined as

$$\mathcal{Y} = \mathbf{C}_{I_1, \dots, I_N} [\mathcal{W}, \mathcal{X}^{(1)}, \mathcal{X}^{(2)}, \dots, \mathcal{X}^{(N)}], \quad (5)$$

where $\mathcal{W} \in \mathbb{R}^{I_1 \times \dots \times I_N \times O}$ is a general N -order weight tensor. Note that the number of trainable parameters scales exponentially as $O(\prod_{n=1}^N I_n)$. To reduce the computation cost,

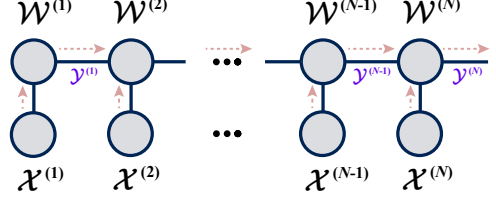


Fig. 3. The TT model that is contracted from left to right. The outputs after the contractions are denoted in a blue font.

\mathcal{W} can be replaced by a set of low-order tensors which is further contracted according to (3). The contraction of TT is equivalent to the feed forward process in neural networks. For example, the red arrows in Fig. 3 indicate a forward direction of TT. The input vector $\mathcal{X}^{(1)}$ is contracted with the weight tensor $\mathcal{W}^{(1)}$ to produce the output tensor $\mathcal{Y}^{(1)} \in \mathbb{R}^{V_1}$. The second weight tensor $\mathcal{W}^{(2)}$ and the second input vector $\mathcal{X}^{(2)}$ are contracted to generate an intermediate matrix $\mathcal{A}^{(2)} \in \mathbb{R}^{V_1, V_2}$, which is then contracted with $\mathcal{Y}^{(1)} \in \mathbb{R}^{V_1}$ to generate the second output tensor $\mathcal{Y}^{(2)} \in \mathbb{R}^{V_2}$. The final output is denoted by $\mathcal{Y}^{(N)} \in \mathbb{R}^O$, whose elements can be written as

$$y_o^{(N)} = \sum_{v_1 \dots v_{N-1}} \sum_{i_1 \dots i_N} w_{i_1 v_1}^{(1)} x_{i_1}^{(1)} \dots w_{i_N v_{N-1}}^{(N)} x_{i_N}^{(N)}, \quad (6)$$

which clearly encodes the N -order interactions among the input features, without low-order terms.

TT can be optimized by gradient descent with respect to the mean squared error. In [12], two nearby tensors are contracted to form a new high-order tensor at each step, and then the gradient is calculated by taking the derivative of the cost function with respect to this tensor. After updating the parameters, a singular value decomposition is performed to restore the updated tensor into two low-order tensors. This method sweeps back and forth along the TT and iteratively minimizes the cost function. Notably, at each step all of the tensor nodes must be contracted, which may involve hundreds of multiplications which may lead to the gradient vanishing or exploding problem. Several procedures must be taken to counteract this effect, e.g., normalizing the input and output at each step, dividing the bond tensor with its largest element, etc. This algorithm has been implemented in the TensorNetwork library [34] which uses TensorFlow as the backend for speeding up the tensor computations.

III. RESIDUAL TENSOR TRAIN

Residual structure is widely used in the design of deep neural networks. In ResNet, the identity mapping enabled by skip connections allows the input signal to propagate directly from one layer to any other layer, which solves the problem of network degradation to a certain extent [35]. Besides, the residual network can be regarded as an ensemble model that consists of a series of path sets [36], thereby improving the robustness of the model. Similar to ResNet, the ResTT is proposed to solve the following issues:

- The plain TT network only models the N -order interaction between all the input features while ignores the

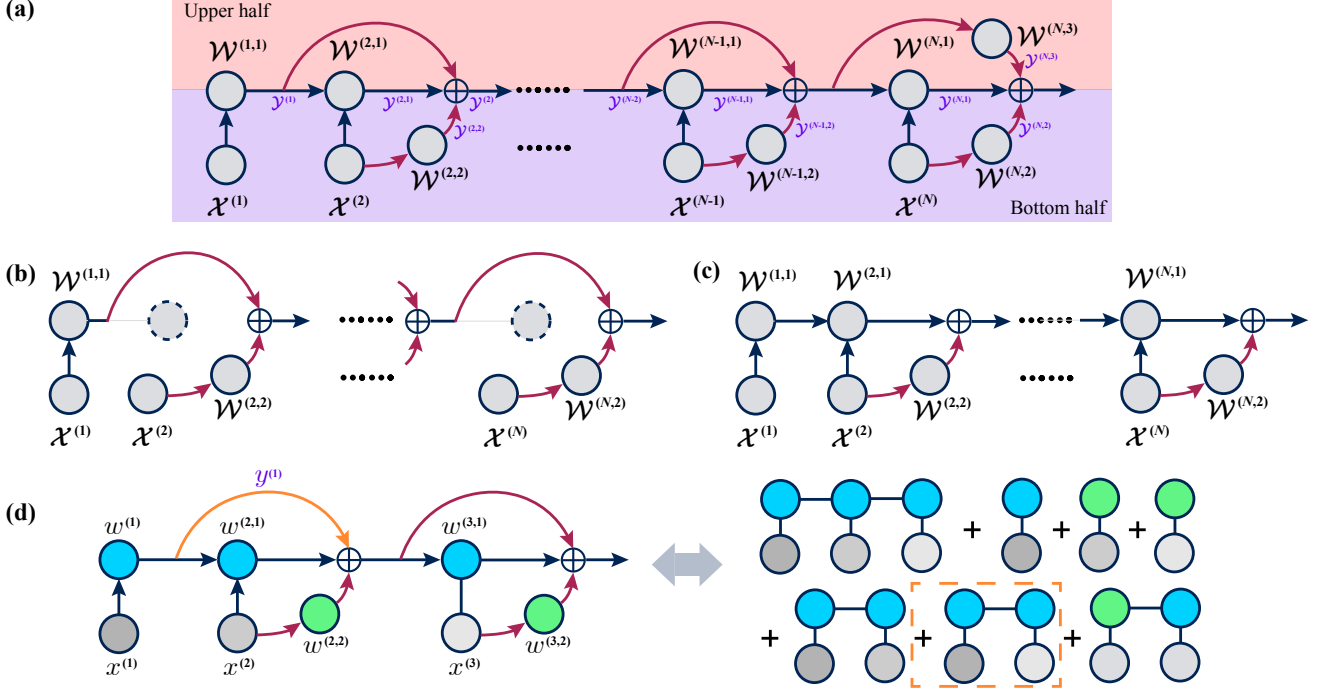


Fig. 4. The graphical representation of ResTT. (a) Pipeline of the general ResTT. At each summing junction, two shortcuts (in red line) are added to the output. The arrows indicate the contraction direction. (b-c) The ResTT forms of an N -node fully-connected layer and the discrete Volterra series up to the N -th order. (d) An example of ResTT with three inputs and its equivalent form.

low-order interactions between a subset of features, such as linear or bilinear correlations. More importantly, the plain TT network lacks the flexibility in designing the combination of feature interactions with different orders as required.

- The current TT models are difficult to train with a large number of tensor nodes. As residual connection has been proven to be effective in stabilizing the training process for very deep neural networks, it can also be added to the TT network to improve its training stability.

A. The General Model

The diagrammatic representation of a general ResTT model is shown in Fig. 4 (a), in which the contractions are conducted from left to right. Firstly, $\mathcal{X}^{(1)}$ is contracted with $\mathcal{W}^{(1,1)}$ to generate the output $\mathcal{Y}^{(1)} \in \mathbb{R}^{V_1}$ by

$$\mathcal{Y}^{(1)} = \mathcal{C}_{I_1}[\mathcal{X}^{(1)}, \mathcal{W}^{(1,1)}]. \quad (7)$$

Then $\mathcal{X}^{(2)}$ is contracted with $\mathcal{Y}^{(1)}$ and $\mathcal{W}^{(2,1)}$ to generate the normal output $\mathcal{Y}^{(2,1)} \in \mathbb{R}^{V_2}$ by

$$\mathcal{Y}^{(2,1)} = \mathcal{C}_{V_1, I_2}[\mathcal{Y}^{(1)}, \mathcal{W}^{(2,1)}, \mathcal{X}^{(2)}]. \quad (8)$$

The virtual bond dimension of the tensor train is assumed to be the same, i.e., $V_1 = V_2 = \dots = V_{N-1} = r$, and thus we can directly add the skip connection $\mathcal{Y}^{(1)}$ to the output $\mathcal{Y}^{(2,1)}$. Besides, $\mathcal{X}^{(2)}$ is contracted with an additional node $\mathcal{W}^{(2,2)} \in \mathbb{R}^{I_2 \times V_2}$ to generate the low-order interaction terms that include the features in the input $\mathcal{X}^{(2)}$, according to the following formula

$$\mathcal{Y}^{(2,2)} = \mathcal{C}_{I_2}[\mathcal{X}^{(2)}, \mathcal{W}^{(2,2)}]. \quad (9)$$

The output of the second layer of ResTT is given by

$$\mathcal{Y}^{(2)} = \mathcal{Y}^{(2,1)} + \mathcal{Y}^{(1)} + \mathcal{Y}^{(2,2)}. \quad (10)$$

Note that the skip connection $\mathcal{Y}^{(1)}$ produces the low-order terms that include features in the input $\mathcal{X}^{(1)}$. By repeating this process we obtain

$$\begin{aligned} \mathcal{Y}^{(n,1)} &= \mathcal{C}_{V_{n-1}, I_n}[\mathcal{Y}^{(n-1)}, \mathcal{W}^{(n,1)}, \mathcal{X}^{(n)}], \\ \mathcal{Y}^{(n,2)} &= \mathcal{C}_{I_n}[\mathcal{X}^{(n)}, \mathcal{W}^{(n,2)}], \\ \mathcal{Y}^{(n)} &= \mathcal{Y}^{(n,1)} + \mathcal{Y}^{(n-1)} + \mathcal{Y}^{(n,2)}. \end{aligned} \quad (11)$$

For the last node a linear mapping is defined by

$$\mathcal{Y}^{(N,3)} = \mathcal{C}_{V_{N-1}}[\mathcal{W}^{(N,3)}, \mathcal{Y}^{(N-1)}] \quad (12)$$

with $\mathcal{W}^{(N,3)} \in \mathbb{R}^{V_{N-1} \times O}$, and the final output of ResTT can be written as

$$\mathcal{Y}^{(N)} = \mathcal{Y}^{(N,1)} + \mathcal{Y}^{(N,3)} + \mathcal{Y}^{(N,2)}. \quad (13)$$

The detailed expression of $\mathcal{Y}^{(N)}$ is given in Appendix A. From the detailed expression, we can see that the output of a general ResTT contains the interaction terms from 1-order (linear) to N -order (N -linear).

B. Special Cases

It is clear from (11) that different connections at each layer generate interaction terms with different orders of features or different input features. Therefore, it is convenient to modify the combination of multilinear terms contained in the final output by adding or deleting the specific connections between the tensor nodes. In particular, many famous models are found

to be special cases of the general ResTT. For example, if only the residual connections shown in Fig. 4 (b) are kept, ResTT will degrade to an N -node fully-connected layer as

$$\mathcal{Y}^{(N)} = \sum_{n=1}^N \mathbf{C}_{I_n}[\mathcal{X}^{(n)}, \mathcal{W}^{(n,2)}]. \quad (14)$$

In this case, the model captures only the linear correlations.

Meanwhile, if we assume the input and output are scalars, i.e., $\mathcal{Y}^{(N)} \in \mathbb{R}$, the general ResTT will degrade to the famous discrete Volterra series [18] when the residual connections in the upper half of Fig. 4 (a) are deleted (See Fig. 4 (c)). The resulting Volterra series are given by

$$\begin{aligned} y = & \sum_{i_N} h_{i_N}^{(N)} x_{i_N}^{(N)} + \sum_{i_N i_{N-1}} h_{i_N i_{N-1}}^{(N-1)} x_{i_N}^{(N)} x_{i_{N-1}}^{(N-1)} + \dots \\ & + \sum_{i_1, \dots, i_N} h_{i_1 \dots i_N}^{(1)} \prod_{j=1}^N x_{i_j}^{(j)} \end{aligned} \quad (15)$$

with

$$\begin{aligned} h_{i_N}^{(N)} &= w_{i_N}^{(N,2)}, \\ h_{i_{N-1} i_N}^{(N-1)} &= \sum_{v_{N-1}} w_{i_{N-1} v_{N-1}}^{(N-1,2)} w_{v_{N-1} i_N}^{(N,1)}, \\ &\dots \\ h_{i_1 \dots i_N}^{(1)} &= \sum_{v_1, \dots, v_{N-1}} w_{i_1 v_1}^{(1,1)} w_{v_1 i_2 v_2}^{(2,1)} \dots w_{i_N v_{N-1}}^{(N,1)} \end{aligned} \quad (16)$$

being the elements of the tensorization form of Volterra kernels denoted by $\mathcal{H}^{(N)} \in \mathbb{R}^{I_N}, \mathcal{H}^{(N-1)} \in \mathbb{R}^{I_N, I_{N-1}}, \dots, \mathcal{H}^{(1)} \in \mathbb{R}^{I_1, I_2, \dots, I_N}$, where the k -order tensor $\mathcal{H}^{(k)}$ is called the k -th Volterra kernel. However, ResTT of this form is difficult to train with respect to a long chain, as the residual connections have been removed. In fact, adding the residual connections can not only stabilize the training process for a large number of nodes (input features), but also enhance the expressive power of Volterra series by introducing additional low-order interaction terms.

In the last, we provide a simple example to further illustrate the flexibility of ResTT. As shown in Fig. 4 (d), the final output of the ResTT can be written as

$$\begin{aligned} y = & w^{(1)} x^{(1)} + w^{(2,2)} x^{(2)} + w^{(3,2)} x^{(3)} + \\ & w^{(1)} w^{(2,1)} x^{(1)} x^{(2)} + w^{(1)} w^{(3,1)} x^{(1)} x^{(3)} + \\ & w^{(2,2)} w^{(3,1)} x^{(2)} x^{(3)} + w^{(1)} w^{(2,1)} w^{(3,1)} x^{(1)} x^{(2)} x^{(3)}. \end{aligned} \quad (17)$$

Suppose the skip connection of $y^{(1)}$ (the orange line in Fig. 4 (d)) has been removed. Then the output of ResTT will change to

$$\begin{aligned} y = & w^{(1)} x^{(1)} + w^{(2,2)} x^{(2)} + w^{(3,2)} x^{(3)} + \\ & w^{(1)} w^{(2,1)} x^{(1)} x^{(2)} + w^{(2,2)} w^{(3,1)} x^{(2)} x^{(3)} \\ & w^{(1)} w^{(2,1)} w^{(3,1)} x^{(1)} x^{(2)} x^{(3)}, \end{aligned} \quad (18)$$

in which the 2-order interaction between the input features $x^{(1)}$ and $x^{(3)}$ is discarded. This is because $x^{(1)}$ and $x^{(3)}$ cannot interact directly without the skip connection.

Algorithm 1 ResTT for Supervised Learning

Input: Features $\mathcal{X}^{(1)} \in \mathbb{R}^{I_1}, \mathcal{X}^{(2)} \in \mathbb{R}^{I_2}, \dots, \mathcal{X}^{(N)} \in \mathbb{R}^{I_N}$;
 Label $\mathcal{Y} \in \mathbb{R}^O$;
Initialize: The number of epochs K ;
 Weight tensors $\mathcal{W}^{(1)} \in \mathbb{R}^{I_1 \times V_1}, \mathcal{W}^{(2,1)} \in \mathbb{R}^{V_1 \times I_2 \times V_2}, \mathcal{W}^{(2,2)} \in \mathbb{R}^{I_2 \times V_2}, \dots, \mathcal{W}^{(N,1)} \in \mathbb{R}^{V_{N-1} \times I_N \times O}, \mathcal{W}^{(N,2)} \in \mathbb{R}^{I_N \times O}, \mathcal{W}^{(N,3)} \in \mathbb{R}^{V_{N-1} \times O}$;
 1: **for** $k = 1, \dots, K$ **do**
 2: $\mathcal{Y}^{(1)} = \mathbf{C}_{I_1}[\mathcal{X}^{(1)}, \mathcal{W}^{(1)}]$.
 3: **for** $n = 2, \dots, N$ **do**
 4: $\mathcal{Y}^{(n,1)} = \mathbf{C}_{V_{n-1}, I_n}[\mathcal{Y}^{(n-1)}, \mathcal{W}^{(n,1)}, \mathcal{X}^{(n)}]$.
 5: $\mathcal{Y}^{(n,2)} = \mathbf{C}_{I_n}[\mathcal{X}^{(n)}, \mathcal{W}^{(n,2)}]$.
 6: **if** $n \neq N$ **then**
 7: $\mathcal{Y}^{(n)} = \mathcal{Y}^{(n,1)} + \mathcal{Y}^{(n-1)} + \mathcal{Y}^{(n,2)}$.
 8: **end if**
 9: **end for**
 10: $\mathcal{Y}^{(N,3)} = \mathbf{C}_{V_{N-1}}[\mathcal{W}^{(N,3)}, \mathcal{Y}^{(N-1)}]$.
 11: $\mathcal{Y}^{(N)} = \mathcal{Y}^{(N,1)} + \mathcal{Y}^{(N,2)} + \mathcal{Y}^{(N,3)}$.
 12: Calculate the cost function: $c(\mathcal{Y}, \mathcal{Y}^{(N)})$.
 13: Update the weight tensors by backpropagation.
 14: **end for**

C. Optimization

Since the operation of tensor contraction is similar to the linear transformation layer of conventional neural networks, we can adopt the standard backpropagation algorithm [37] to optimize the ResTT. Here we briefly show the gradient calculation of the weight tensor $\mathcal{W}^{(k,1)}$ as follows

$$\begin{aligned} \Delta \mathcal{W}^{(k,1)} &= - \frac{\partial c}{\partial \mathcal{W}^{(k,1)}} \\ &= - \frac{\partial c}{\partial \mathcal{Y}^{(N)}} \cdot \frac{\partial \mathcal{Y}^{(N)}}{\partial \mathcal{Y}^{(N-1)}} \cdot \frac{\partial \mathcal{Y}^{(N-1)}}{\partial \mathcal{Y}^{(N-2)}} \dots \frac{\partial \mathcal{Y}^{(k)}}{\partial \mathcal{W}^{(k,1)}} \\ &= - \frac{\partial c}{\partial \mathcal{Y}^{(N)}} \cdot (\mathcal{I} + \mathcal{A}^{(N)}) \dots \frac{\partial \mathcal{Y}^{(k)}}{\partial \mathcal{W}^{(k,1)}} \\ &= - \frac{\partial c}{\partial \mathcal{Y}^{(N)}} \cdot (\mathcal{I} + \mathcal{A}^{(N)}) \dots (\mathcal{I} + \mathcal{A}^{(k+1)}) \\ &\quad \otimes \mathcal{X}^{(k)} \otimes \mathcal{Y}^{(k-1)}, \end{aligned} \quad (19)$$

with the intermediate matrix $\mathcal{A}^{(k)}$ whose elements are given by

$$a_{v_k v_{k-1}}^{(k)} = \sum_{i_k} w_{v_k i_k v_{k-1}}^{(k,1)} x_{i_k}. \quad (20)$$

Here \mathcal{I} is an $r \times r$ identity matrix and c is the current value of the cost function. Dot notation \cdot in (19) means that the derivatives are connected by matrix multiplication along the compatible indices. Similarly, the gradient of the weight tensor

$\mathcal{W}^{(k,2)}$ is given by

$$\begin{aligned}\Delta\mathcal{W}^{(k,2)} &= -\frac{\partial c}{\partial\mathcal{W}^{(k,2)}} \\ &= -\frac{\partial c}{\partial\mathcal{Y}^{(N)}} \cdot \frac{\partial\mathcal{Y}^{(N)}}{\partial\mathcal{Y}^{(N-1)}} \cdot \frac{\partial\mathcal{Y}^{(N-1)}}{\partial\mathcal{Y}^{(N-2)}} \cdots \frac{\partial\mathcal{Y}^{(k)}}{\partial\mathcal{W}^{(k,2)}} \\ &= -\frac{\partial c}{\partial\mathcal{Y}^{(n)}} \cdot (\mathcal{I} + \mathcal{A}^{(N)}) \cdots (\mathcal{I} + \mathcal{A}^{(k)}) \otimes \mathcal{X}^{(k)}.\end{aligned}\quad (21)$$

The details of the ResTT implementation for supervised learning are summarized in Algorithm 1.

D. Complexity Analysis

Here we compare the memory complexity and time complexity of three multilinear models, including the fully general tensorized model in (5), the plain TT in (3) and ResTT. The memory complexity of (5) is $O(\prod_{n=1}^N i_k)$. In contrast, the memory complexities of TT and ResTT are $O(\sum_{n=1}^N I_n r^2)$ and $O(\sum_{n=1}^N (I_n r^2 + I_n r))$, respectively. The time complexities for TT and ResTT are $O(\sum_{n=1}^N I_n r^3)$ and $O(\sum_{n=1}^N (I_n r^3 + I_n r))$, respectively, while (5) has a complexity of $O(\prod_{n=1}^N I_k)$.

IV. MEAN-FIELD ANALYSIS

Mean-field analysis [19], [38] provides an efficient way to assess the training stability of a deep learning neural network. In this paper we extend this analysis to study the characteristics of signal propagations in TT and ResTT. First we assume that all the weights in TT and ResTT are initialized from the same Gaussian distribution $\mathcal{N}(0, \sigma_w^2/r)$, and then calculate the evolution of the variances of the outputs $\{\mathcal{Y}^{(k)}\}$ and the average magnitude of the gradients. The detailed derivations are given in Appendix B.

A. Tensor Train

As all the weights are *i.i.d* with zero mean, the output $\mathcal{Y}^{(k)}$ satisfies

$$\mathbb{E}(y_{v_k}^{(k)}) = 0, \quad (22)$$

and the variance of the output, denoted by $q^{(k)}$, is calculated as

$$q^{(k)} = \mathbb{E}\left(\sum_{i_k} (x_{i_k}^{(k)})^2\right) \sigma_w^2 q^{(k-1)} = s^{(k)} q^{(k-1)}, \quad (23)$$

with $s^{(k)} = \mathbb{E}\left(\sum_{i_k} (x_{i_k}^{(k)})^2\right) \sigma_w^2$. Hence, the relation between the input- and output- variances at each layer is characterized by the slope factor $s^{(k)}$. As can be seen from (23), the slope factor is influenced by the variance of the input data, which is significantly different from the conventional deep learning model where the evolution of the output at each layer can only be influenced by the variance of the weights. In addition, the backward propagation in TT is studied by calculating the input-output Jacobian, which relates the gradients to the weight tensor at a given position. The Jacobian for the input $\mathcal{Y}^{(k-1)}$ is denoted by $\mathcal{J}^{(k)} \in \mathbb{R}^{V_{k-1} \times I_k \times V_k}$ and calculated as

$$\mathcal{J}^{(k)} = \frac{\partial\mathcal{Y}^{(N)}}{\partial\mathcal{Y}^{(N-1)}} \cdots \frac{\partial\mathcal{Y}^{(k)}}{\partial\mathcal{Y}^{(k-1)}} = \mathcal{A}^{(N)} \cdots \mathcal{A}^{(k+1)} \otimes \mathcal{X}^{(k)}$$

with the intermediate matrix $\mathcal{A}^{(k)}$ defined in (20). The quadratic mean $\chi^{(k)}$ of the elements in the Jacobian characterizes the magnitude of the gradients in backpropagation, which is given by

$$\chi^{(k)} = s^{(k)} \chi^{(k+1)}. \quad (24)$$

According to (23) and (24), the signals in the forward- and backward- propagations will explode in a long TT when $s^{(k)} > 1$. In contrast, if $s^{(k)} < 1$, the signals will tend to vanish. Therefore, the condition of stability for the training is given by the following formula

$$s^{(k)} = 1, \quad k \geq 1. \quad (25)$$

Since the $s^{(k)}$ is determined by the input data, we have to preprocess the input in order to stabilize the training. For example, by employing the trigonometric mapping [39] to the input and transforming the feature vector $\mathcal{X}^{(k)}$ as

$$\phi(\mathcal{X}^{(k)}) = \frac{1}{\sqrt{I_k}} [\cos(\frac{\pi}{2} \mathcal{X}^{(k)}), \sin(\frac{\pi}{2} \mathcal{X}^{(k)})], \quad (26)$$

we have $\mathbb{E}(\sum_{i_k} (x_{i_k}^{(k)})^2) = 1$. Then (25) can be satisfied by letting $\sigma_w^2 = 1$. In this case we get

$$q^{(k)} = q^{(k-1)}, \quad \chi^{(k)} = \chi^{(k+1)}, \quad (27)$$

which is the critical condition for the stable training of TT.

B. Residual Tensor Train

In ResTT, the k -th output vector also satisfies $\mathbb{E}(y_{v_k}^{(k)}) = 0$, and the variance of this vector is calculated as

$$q^{(k)} = (s^{(k)} + 1)q^{(k-1)} + s^{(k)}. \quad (28)$$

In backward propagation, the quadratic mean of the input-output Jacobian for the input $\mathcal{Y}^{(k-1)}$ is calculated as

$$\chi^{(k)} = (s^{(k)} + 1)\chi^{(k+1)}, \quad (29)$$

which shares the same slope factor as the forward propagation. Hence, $(s^{(k)} + 1)$ determines the evolution of the signals in the training of ResTT. Note that for any choice of σ_w^2 , $(s^{(k)} + 1)$ is always larger than 1, which means the signals in the forward and backward propagation will never vanish. Meanwhile, in order to prevent the signals from exploding, the following condition has to be satisfied

$$s^{(k)} \ll 1. \quad (30)$$

According to (23), as long as $\sigma_w^2 \ll 1$, the condition of stability (30) will be satisfied given that the variance of the input data is bounded. Compared to TT which requires $\mathbb{E}(\sum_{i_k} (x_{i_k}^{(k)})^2) \sigma_w^2 = 1$, the condition $\sigma_w^2 \ll 1$ is significantly relaxed.

V. EXPERIMENTS

We conduct experiments on several datasets, including a synthetic dataset, MNIST dataset and Fashion-MNIST dataset. In terms of experimental setup, we optimize the models by Adam optimizer [40]. The learning rate is chosen from $\{1e^{-2}, 1e^{-3}, 1e^{-4}\}$. All models are trained for 100 epochs. We fix the mini-batch size as 512 and set the weight decay as $1e^{-6}$ for all tasks. The implementations are based on Pytorch [41] and the models are trained on NVIDIA GTX 1080Ti.

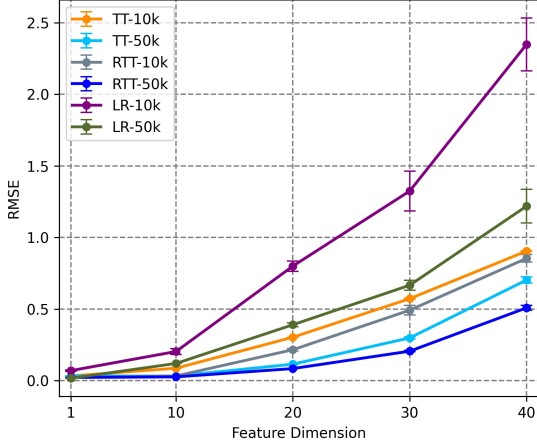


Fig. 5. Comparisons between ResTT, TT and LR on synthetic datasets with different data sizes. The Y-axis is RMSE and X-axis is the dimension of feature. ResTT- N is the notation for the ResTT model that trains on N samples.

A. Synthetic dataset

In order to verify the capability of ResTT in modelling multiple multilinear feature interactions, we generate the synthetic dataset by

$$\hat{y} = \sum_{i=1}^d w_i^{(1)} x_i^{(1)} + \sum_{i,j=1}^d w_{ij}^{(2)} x_i^{(1)} x_j^{(2)} + \sum_{i,j,k=1}^d w_{ijk}^{(3)} x_i^{(1)} x_j^{(2)} x_k^{(3)}, \quad (31)$$

where the elements of $\mathcal{W}^{(1)} \in \mathbb{R}^d$, $\mathcal{W}^{(2)} \in \mathbb{R}^{d \times d}$, $\mathcal{W}^{(3)} \in \mathbb{R}^{d \times d \times d}$ are randomly sampled from $\mathcal{N}(0, 0.1)$, and $\mathcal{X}^{(1)}, \mathcal{X}^{(2)}, \mathcal{X}^{(3)} \in \mathbb{R}^d$ are randomly sampled from $\mathcal{N}(0, 0.5)$. The training size is selected from $\{10000, 50000\}$ while the test size is 10000 for all cases. The feature dimension d is selected from $\{1, 10, 20, 30, 40\}$. We conduct experiments on TT ($r = 20$), ResTT ($r = 20$) and the Linear Regression (LR) model. Each model has been run 5 times to average the effect of random initialization.

We use the Root Mean Square Error (RMSE) as the evaluation metric. The results are shown in Fig. 5. It is clear that LR model cannot extract the complex multilinear correlations from the synthetic data. TT performs better than LR, with its ability to model high-order feature interaction instead of the low-order ones. Nevertheless, the performance achieved by TT is still worse than the performance of ResTT, which is able to model a comprehensive set of feature interactions. Fig. 5 also shows that the advantage of ResTT over TT and LR is getting more dominant with the increase of feature dimension d . In that case, LR and TT, which only model 1-order and N -order interactions, are unable to capture the large number of correlations in (31).

B. Image classification

1) Datasets:

TABLE I
THE NUMBER OF TRAINABLE PARAMETERS FOR TT AND ResTT WITH DIFFERENT VIRTUAL BOND DIMENSIONS r ON THE MNIST AND FASHION-MNIST DATASETS.

r	TT	ResTT
10	38840	42740
20	155280	163080
30	349320	361020
40	620960	636560
50	970200	989700
100	3880400	3919400

TABLE II
COMPARISONS OF THE CLASSIFICATION ACCURACY (%) OF ResTT AND MEANTT WITH THE STATE-OF-THE-ART TENSOR NETWORK MODELS ON THE TEST SETS OF MNIST AND FASHION-MNIST.

Model	MNIST	Fashion-MNIST
TTN [31]	95%	–
MPS [34]	98%	88%
EPS-SBS [32]	98.7%	88.6%
Snake-SBS [32]	99%	89.2%
TT-B($r = 100$)	95.05%	85.68%
MeanTT($r = 100$)	98.75%	88.86%
ResTT($r = 100$)	99.04%	89.95%
Linear SVC [21]	91.7%	83.6%
LR [21]	91.7%	84.2%
MLP [21]	97.2%	87.1%
AlexNet [32]	98.97%	89.9%

- a) *MNIST*: The MNIST is a dataset of handwritten digits from 0 to 9, which contains 60,000 training samples and 10,000 testing samples with 28×28 gray-scale pixels. Each pixel takes integer in the range $[0, 255]$. Following [12], each pixel value of the image is normalized to $[0, 1]$ and mapped into a two-dimensional space by a trigonometric function defined in (26). Hence, each feature of this task is a 2-dimensional vector. Meanwhile, images are scaled down to 14×14 by averaging the clusters of four adjacent pixels.
- b) *Fashion-MNIST*: The Fashion-MNIST [21] is a dataset of Zalando's article images, which consists of a training set of 60,000 samples and a test set of 10,000 samples. Each image is a 28×28 gray-scale image, associated with a label from 10 classes. Similar to MNIST, each pixel value is normalized to $[0, 1]$ and mapped to a two-dimensional space by the trigonometric function. Each image is scaled down to 14×14 by averaging the clusters of four adjacent pixels.

2) *Model*: The following tensor network models are tested in the experiments:

- a) *MPS* [12]: Matrix Product State (MPS) is a special TT model in which all the tensor nodes are kept unitary and trained by the DMRG-like optimization algorithm.
- b) *TTN* [31]: Tree tensor network is a 2-layer tensor network model that supports hierarchical feature extraction, which uses a training algorithm derived from the multipartite entanglement renormalization ansatz.

TABLE III
TEST ACCURACY (%) W.R.T. THE FRACTION OF THE TRAINING SAMPLES ON MNIST AND FASHION-MNIST DATASETS.

Dataset	Method	r	Parm.	Training 1%	Training 5%	Training 10%	Training 20%	Training 50%	Training 100%
MNIST	MeanTT	20	0.15M	30.16±14.59	37.03±14.95	48.53±26.75	68.14±20.70	57.01±33.17	38.54±33.14
	MeanTT	100	3.88M	85.87±0.6054	94.57±0.1231	96.20±0.1762	97.27±0.0721	98.36±0.0412	98.70±0.0474
	ResTT	20	0.16M	89.52±0.2917	95.19±0.1088	96.49±0.0889	97.41±0.0902	98.34±0.0306	98.53±0.0397
	ResTT	100	3.92M	89.82±0.2755	95.46±0.0768	96.74±0.0706	97.68±0.0687	98.66±0.0329	98.96±0.0304
Fashion-MNIST	MeanTT	20	0.15M	22.77±1.071	30.72±0.5816	53.11±0.1682	44.67±0.1979	56.29±0.0804	37.44±0.1035
	MeanTT	100	3.88M	77.07±0.4257	82.72±0.2014	84.39±0.1861	85.92±0.1282	87.66±0.0986	88.79±0.0841
	ResTT	20	0.16M	75.48±0.4455	82.11±0.2052	83.95±0.0925	85.45±0.0731	86.95±0.0695	87.95±0.0913
	ResTT	100	3.92M	78.86±0.3120	84.18±0.1554	85.69±0.1116	87.16±0.1363	88.93±0.1132	89.85±0.1064

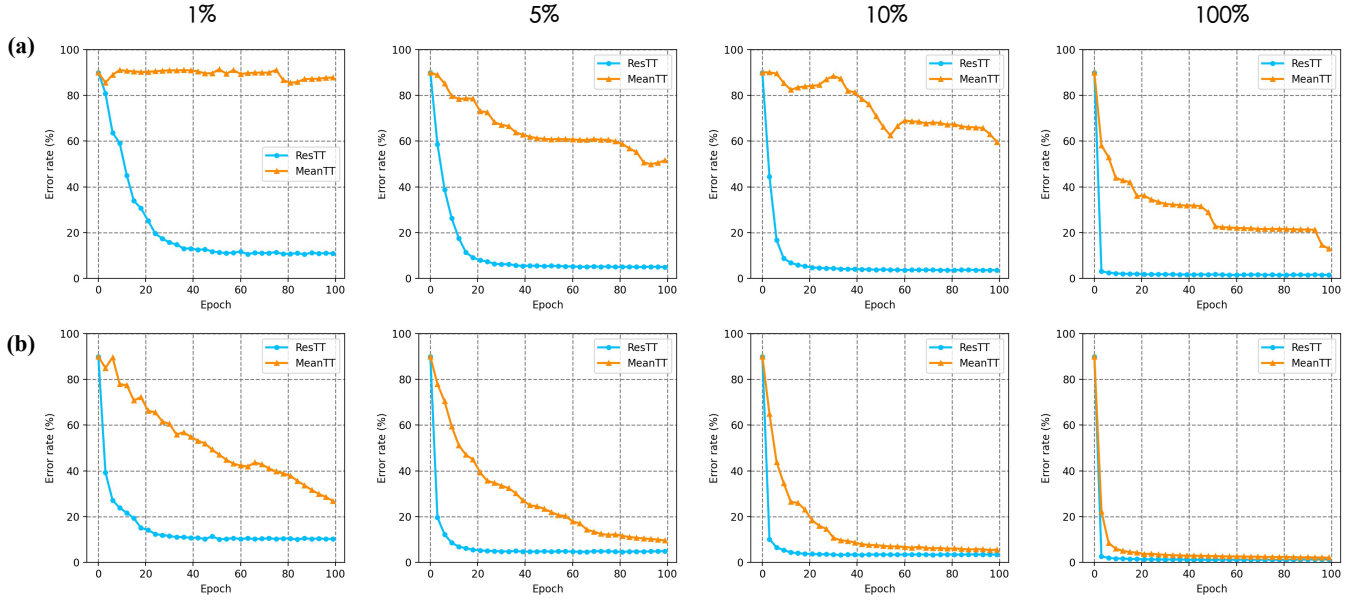


Fig. 6. Test accuracy of ResTT (blue curve) and MeanTT (orange curve) versus the training epochs on MNIST. (a), (b) are the model performances with $r = 20$ and $r = 100$, respectively.

- c) *EPS-SBS* [32]: Entangled Plaquette State (EPS) is defined as a product of tensors on overlapping clusters of variables and String-Bond State (SBS) is defined by placing MPS over strings on a graph which needs not to be a one-dimensional lattice. EPS-SBS is a tensor network that consists of an EPS followed by a SBS and optimized by stochastic gradient descent.
- d) *Snake-SBS* [32]: Snake-SBS consists of four overlapping SBS structures in a snake pattern and is optimized by stochastic gradient decent.
- e) *TT-BN*: Tensor train with Batch Normalization (BN). In this model, a BN layer [42] is added after each contraction. TT-BN is trained by backpropagation.
- f) *MeanTT*: Mean-field Tensor Train is the vanilla TT model which is initialized using the stability condition derived in Sec. IV-A. MeanTT is trained by backpropagation.

Other models for comparison are listed in the following:

- a) *Linear-SVC*: Linear Support Vector Classification is a kernel method that aims to construct a series of hyperplanes in the linear feature space to classify samples.
- b) *LR*: Linear regression is a statistical model that captures

- the linear correlation of the input features.
- c) *MLP*: Multi-Layer Perceptron is a type of feed-forward neural network that consists of multiple fully-connected layers (with threshold activation). With the high-level features extracted by the hierarchical structure, MLP is able to distinguish data that is not linearly separable. The MLP tested here is adopted from [21], which is composed of two layers with 100 hidden neurons and ReLU activation.
- d) *AlexNet*: AlexNet is one of the most influential convolutional neural network model proposed in [43]. AlexNet is built by 5 convolutional layers and 3 fully-connected layers, which employs some of the most effective regularization techniques such as dropout, pooling and ReLU activation.

- 3) *Results*: Table I shows that the additional connections in the ResTT do not introduce a significant amount of parameters, which means TT and ResTT can be compared with the same virtual bond dimension r . This is because most of the parameters are contained in the high-order tensors generated by $\{\mathcal{W}^{(n,1)}\}$, while the additional parameters are

contained in $\{\mathcal{W}^{(n,2)}\}$ which only generate low-order tensors. The test accuracy on MNIST and Fashion-MNIST datasets are presented in Table II. It can be observed that ResTT outperforms all the state-of-the-art tensor network models on both MNIST and Fashion-MNIST datasets. In particular, MeanTT achieves better test accuracy than the regularized MPS and TT-BN, which indicates that proper initialization of the weights can lead to improved performance without any regularization techniques. Besides, the performance of ResTT is much better than that of linear SVC and LR. The test accuracy of ResTT with less than 4M parameters ($r = 100$) is slightly higher than the famous AlexNet, while AlexNet has 60M parameters.

Next, we conduct multiple sets of experiments by choosing r in $\{20, 50, 100\}$ and varying the fraction of data for training by $\{1\%, 5\%, 10\%, 20\%, 50\%, 100\%\}$. Each model has been run 10 times to average the effect of random initialization. The mean and standard deviation of the test accuracy are reported in Table III. When the fraction is 1%, that is, only 600 randomly selected samples are used for training, ResTT can achieve an error rate of 10.18% on the test set which contains 10000 test samples. In this case, ResTT not only significantly outperforms MeanTT, but also beats the multi-task learning methods for limited data that were proposed in [22], namely Deep Multi-Task Representation Learning based on Tensor Train (DMTRL-TT) ($\sim 13\%$), DMTRL-Tucker ($\sim 17\%$) and DMTRL-LAF ($\sim 15\%$) on the MNIST dataset.

Moreover, it is worth mentioning that ResTT converges much faster than MeanTT. As can be seen from Fig. 6, the training of MeanTT with $r = 20$ is highly unstable on a fraction of data, while ResTT can converge to an approximately optimal point within just 20 epoches. In Fig. 6 (b), ResTT with $r = 100$ takes only about 5 epoches to complete the training. According to the numerical results, ResTT consistently outperforms MeanTT in terms of the training stability and test accuracy, even if we have shown that MeanTT is already more stable in training than other tensor network models such as regularized MPS and TT-BN. Therefore, it is clear that the residual connections, with proper initialization guided by the mean-field analysis, can indeed improve the effectiveness and training stability of the model.

VI. CONCLUSION

In this paper, we propose a general framework that combines residual connections with TT to model feature interactions, from 1-order to N -order, within one model. Mean-field analysis has been extended to TT and ResTT to derive the condition of stability for the initialization of deep tensor networks. In particular, the stability condition of ResTT is significantly relaxed due to the residual connections. ResTT has demonstrated significant improvement in training stability and convergence speed over the plain TT.

Numerical experiments on the synthetic, MNIST and Fashion-MNIST datasets have shown the advantage of ResTT in capturing multiple multilinear correlations. The future direction would be to evaluate these tools on more practical and complex problems in which high-order multimodal correlations naturally exist. For example, it would be interesting to

explore the application of ResTT in multi-task learning and continual learning models, for which the high-order feature interaction is often adopted. As ResTT can be seen as an enhanced version of Volterra series, we also anticipate its applications in the learning with sequential data.

APPENDIX A DETAILED EXPRESSION OF THE OUTPUT OF A GENERAL RESTT

The elements of the final output of the ResTT with N input features are calculated in the following, ranked from high-order to low-order. Firstly, the N -order term is calculated to be

$$\sum_{v_1, \dots, v_{N-1}} \sum_{i_1, \dots, i_N} w_{i_1 v_1}^{(1,1)} w_{i_2 v_2}^{(2,1)} \dots w_{i_N v_N}^{(N,1)} x_{i_1}^{(1)} \dots x_{i_N}^{(N)}. \quad (32)$$

This term is the output of a plain TT network. Secondly, the $(N-1)$ -order terms are calculated to be

$$\begin{aligned} & \sum_{v_2, \dots, v_{N-1}} \sum_{i_2, \dots, i_N} w_{i_2 v_2}^{(2,2)} \dots w_{i_N v_N}^{(N,1)} \\ & \quad x_{i_2}^{(2)} \dots x_{i_N}^{(N)}, \\ & \quad \dots \\ & \sum_{v_1, \dots, v_{k-1}, v_{k+1}, \dots, v_{N-1}} \sum_{i_1, \dots, i_{k-1}, i_{k+1}, \dots, i_N} \\ & \quad w_{i_1 v_1}^{(1)} \dots w_{i_{k-1} v_{k-1}}^{(k-1,2)} w_{v_{k-1} i_{k+1} v_{k+1}}^{(k+1,1)} \dots w_{v_{N-1} v_N}^{(N)} \\ & \quad x_{i_1}^{(1)} \dots x_{i_{k-1}}^{(k-1)} x_{i_{k+1}}^{(k+1)} \dots x_{i_N}^{(N)}, \\ & \quad \dots \\ & \sum_{v_1, \dots, v_{N-2}} \sum_{i_1, \dots, i_{N-1}} w_{i_1 v_1}^{(1,1)} \dots w_{v_{N-1} v_N}^{(N,3)} \\ & \quad x_{i_1}^{(1)} \dots x_{i_{N-1}}^{(N-1)}. \end{aligned} \quad (33)$$

Similarly, the $(N-2)$ -order terms can be calculated as

$$\begin{aligned} & \sum_{v_3, \dots, v_{N-1}} \sum_{i_3, \dots, i_N} w_{i_3 v_3}^{(3,2)} w_{i_4 v_4}^{(4,1)} \dots w_{v_{N-1} i_N v_N}^{(N)} \\ & \quad x_{i_3}^{(3)} \dots x_{i_N}^{(N)}, \\ & \quad \dots \\ & \sum_{v_1, \dots, v_{k-1}, v_{k+2}, \dots, v_{N-1}} \sum_{i_1, \dots, i_{k-1}, i_{k+2}, \dots, i_N} \\ & \quad w_{i_1 v_1}^{(1)} \dots w_{i_{k-1} v_{k-1}}^{(k-1,2)} w_{v_{k-1} i_{k+2} v_{k+2}}^{(k+2,1)} \dots w_{v_{N-1} i_N v_N}^{(N,1)} \\ & \quad x_{i_1}^{(1)} \dots x_{i_{k-1}}^{(k-1)} x_{i_{k+2}}^{(k+2)} \dots x_{i_N}^{(N)}, \\ & \quad \dots \\ & \sum_{v_1, \dots, v_{N-2}} \sum_{i_1, \dots, i_{N-2}} w_{i_1 v_1}^{(1,1)} \dots w_{v_{N-2} v_N}^{(N,3)} \\ & \quad x_{i_1}^{(1)} \dots x_{i_{N-2}}^{(N-2)}. \end{aligned} \quad (34)$$

The rest of the interaction terms can be obtained in the same manner. Finally, we have the following 1-order terms (linear correlations)

$$\sum_{i_1} w_{i_1 v_N}^{(1,1)} x_{i_1}^{(1)}, \sum_{i_2} w_{i_2 v_N}^{(2,2)} x_{i_2}^{(2)}, \dots, \sum_{i_N} w_{i_N v_N}^{(N,2)} x_{i_N}^{(N)}. \quad (35)$$

The final output of ResTT is the summation of all terms, from 1-order (linear) to N -order (N -linear).

APPENDIX B MEAN-FIELD ANALYSIS OF TT AND RESTT

Recall that all the weights are initialized from the same Gaussian distribution $\mathcal{N}(0, \sigma_w^2/r)$. We have

$$\mathbb{E}(y_{v_k}^{(k)}) = 0. \quad (36)$$

Then the variance of the k -th output vector is

$$q^{(k)} = \mathbb{E}\left[\left(\sum_{v_{k-1}, i_k} y_{v_{k-1}}^{(k-1)} w_{v_{k-1} i_k v_k}^{(k)} x_{i_k}^{(k)}\right)^2\right]. \quad (37)$$

Since $y_{v_{k-1}}^{(k-1)}, w_{v_{k-1} i_k v_k}^{(k)}, x_{i_k}^{(k)}$ are independent, we have

$$\mathbb{E}[y_{v_{k-1}}^{(k-1)} w_{v_{k-1} i_k v_k}^{(k)} x_{i_k}^{(k)}] = 0. \quad (38)$$

Hence, (37) can be simplified as

$$\begin{aligned} q^{(k)} &= \mathbb{E}\left[\sum_{v_{k-1}, i_k} (y_{v_{k-1}}^{(k-1)})^2 (w_{v_{k-1} i_k v_k}^{(k)})^2 (x_{i_k}^{(k)})^2\right] \\ &= \mathbb{E}\left[\sum_{i_k} (x_{i_k}^{(k)})^2\right] \sigma_w^2 q^{(k-1)}. \end{aligned} \quad (39)$$

Similarly, the derivations of quadratic mean $\chi^{(k)}$ of the elements in $\mathcal{J}^{(k)}$ are given by

$$\begin{aligned} \chi^{(k)} &= \frac{1}{r} \mathbb{E}\left(\sum_{v_{k-1}} (j_{v_{k-1}}^{(k)})^2\right) = \frac{1}{r} \mathbb{E}\left(\sum_{v_{k-1}} (j^{(k+1)} \cdot a^{(k)})_{v_{k-1}}^2\right) \\ &= \frac{1}{r} \mathbb{E}\left[\sum_{v_k, v_{k-1}, i_k} (j_{v_k}^{(k+1)})^2 (a_{v_k v_{k-1}}^{(k)})^2\right] \\ &= \frac{1}{r} \mathbb{E}\left[\sum_{v_k, v_{k-1}, i_k} (j_{v_k}^{(k+1)})^2 (w_{v_k i_k v_{k-1}}^{(k)})^2 (x_{i_k}^{(k)})^2\right] \\ &= \mathbb{E}\left(\sum_{i_k} (x_{i_k}^{(k)})^2\right) \sigma_w^2 \chi^{(k+1)} \end{aligned} \quad (40)$$

The evolution of signals in ResTT is slightly different due to the residual terms. Given that

$$\mathcal{Y}^{(k)} = \mathcal{Y}^{(k,1)} + \mathcal{Y}^{(k,2)} + \mathcal{Y}^{(k-1)}, \quad (41)$$

we have

$$\begin{aligned} q^{(k)} &= \frac{1}{r} \mathbb{E}\left(\sum_{v_k, v_{k-1}, i_k} (y_{v_{k-1}}^{(k-1)})^2 (w_{v_{k-1} i_k v_k}^{(k,1)})^2 (x_{i_k}^{(k)})^2\right) \\ &\quad + \frac{1}{r} \mathbb{E}\left(\sum_{i_k, v_k} (x_{i_k}^{(k)})^2 (w_{i_k v_k}^{(k,2)})^2\right) + \frac{1}{r} \mathbb{E}\left(\sum_{v_{k-1}} (y_{v_{k-1}}^{(k-1)})^2\right) \\ &= (\sigma_w^2 \mathbb{E}\left(\sum_{i_k} (x_{i_k}^{(k)})^2\right) + 1) q^{(k-1)} + \sigma_w^2 \mathbb{E}\left(\sum_{i_k} (x_{i_k}^{(k)})^2\right) \\ &= (s^{(k)} + 1) q^{(k-1)} + s^{(k)}, \end{aligned} \quad (42)$$

and

$$\begin{aligned} \chi^{(k)} &= \frac{1}{r} \mathbb{E}\left(\sum_{v_k, v_{k-1}} (j_{v_k}^{(k)})^2 (a_{v_k v_{k-1}}^{(k,1)})^2 + 1\right)^2 \\ &= \frac{1}{r} \mathbb{E}\left(\sum_{v_k, v_{k-1}, i_k} (j_{v_k}^{(k+1,1)})^2 [(w_{v_k i_k v_{k-1}}^{(k,1)})^2 (x_{i_k}^{(k)})^2 + 1]\right) \\ &= (s^{(k)} + 1) \chi^{(k+1)}. \end{aligned} \quad (43)$$

REFERENCES

- [1] D. A. Freedman, *Statistical models: theory and practice*. Cambridge University Press, 2009.
- [2] I. Steinwart and A. Christmann, *Support vector machines*. Springer Science & Business Media, 2008.
- [3] B. Everitt and A. Skrondal, *The Cambridge Dictionary of Statistics*. Cambridge University Press, 2010.
- [4] J. B. Tenenbaum and W. T. Freeman, “Separating style and content with bilinear models,” *Neural computation*, vol. 12, no. 6, pp. 1247–1283, 2000.
- [5] T.-Y. Lin, A. RoyChowdhury, and S. Maji, “Bilinear cnn models for fine-grained visual recognition,” in *Proc. IEEE conf. CVPR*, Jun. 2015, pp. 1449–1457.
- [6] Y. Gao, O. Beijbom, N. Zhang, and T. Darrell, “Compact bilinear pooling,” in *Proc. IEEE conf. CVPR*, Jun. 2016, pp. 317–326.
- [7] H. Zheng, J. Fu, Z.-J. Zha, and J. Luo, “Looking for the devil in the details: Learning trilinear attention sampling network for fine-grained image recognition,” in *Proc. IEEE conf. CVPR*, Jun. 2019, pp. 5012–5021.
- [8] T. Do, T.-T. Do, H. Tran, E. Tjiputra, and Q. D. Tran, “Compact trilinear interaction for visual question answering,” in *Proc. ICCV*, Nov. 2019, pp. 392–401.
- [9] J. C. Bridgeman and C. T. Chubb, “Hand-waving and interpretive dance: an introductory course on tensor networks,” *Journal of Physics A: Mathematical and Theoretical*, vol. 50, no. 22, p. 223001, 2017.
- [10] G. Evenbly and G. Vidal, “Tensor network states and geometry,” *Journal of Statistical Physics*, vol. 145, no. 4, pp. 891–918, 2011.
- [11] S. Montangero, Montangero, and Evenson, *Introduction to Tensor Network Methods*. Springer, 2018.
- [12] E. Stoudenmire and D. J. Schwab, “Supervised learning with tensor networks,” in *Proc. NIPS*, Dec. 2016, pp. 4799–4807.
- [13] Y. Xu, Z. Wu, J. Chanussot, and Z. Wei, “Hyperspectral images super-resolution via learning high-order coupled tensor ring representation,” *IEEE Transactions on Neural Networks and Learning Systems*, vol. 31, no. 11, pp. 4747–4760, 2020.
- [14] Y. Liu, J. Liu, and C. Zhu, “Low-rank tensor train coefficient array estimation for tensor-on-tensor regression,” *IEEE Transactions on Neural Networks and Learning Systems*, vol. 31, no. 12, pp. 5402–5411, 2020.
- [15] A. Novikov, M. Trofimov, and I. V. Oseledets, “Exponential machines,” in *Proc. ICLR*, Apr. 2017.
- [16] K. He, X. Zhang, S. Ren, and J. Sun, “Deep residual learning for image recognition,” in *Proc. IEEE CVPR*, Jun. 2016, pp. 770–778.
- [17] Y. LeCun, Y. Bengio, and G. Hinton, “Deep learning,” *Nature*, vol. 521, no. 7553, pp. 436–444, 2015.
- [18] S. Boyd and L. Chua, “Fading memory and the problem of approximating nonlinear operators with volterra series,” *IEEE Transactions on Circuits and Systems*, vol. 32, no. 11, pp. 1150–1161, 1985.
- [19] A. M. Saxe, J. L. McClelland, and S. Ganguli, “Exact solutions to the nonlinear dynamics of learning in deep linear neural networks,” in *Proc. ICLR*, May 2014.
- [20] Y. LeCun and C. Cortes, “MNIST handwritten digit database,” 2010. [Online]. Available: <http://yann.lecun.com/exdb/mnist/>
- [21] H. Xiao, K. Rasul, and R. Vollgraf, “Fashion-mnist: a novel image dataset for benchmarking machine learning algorithms,” *arXiv preprint arXiv:1708.07747*, 2017.
- [22] Y. Yang and T. Hospedales, “Deep multi-task representation learning: A tensor factorisation approach,” in *Proc. ICLR*, Apr. 2017.
- [23] Y. Dodge and D. Commenges, *The Oxford dictionary of statistical terms*. Oxford University Press on Demand, 2006.
- [24] S. Weisberg, *Applied linear regression*. John Wiley & Sons, 2005, vol. 528.
- [25] R. Socher, D. Chen, C. D. Manning, and A. Ng, “Reasoning with neural tensor networks for knowledge base completion,” in *Proc. NIPS*, Dec. 2013, pp. 926–934.
- [26] X. Qiu and X. Huang, “Convolutional neural tensor network architecture for community-based question answering,” in *Conf. IJCAI*, Jul. 2015.
- [27] K. Lin, J. Xu, I. M. Baytas, S. Ji, and J. Zhou, “Multi-task feature interaction learning,” in *Proc. ACM SIGKDD*, Aug. 2016, pp. 1735–1744.
- [28] H. Lu, K. N. Plataniotis, and A. N. Venetsanopoulos, “MPCA: Multilinear principal component analysis of tensor objects,” *IEEE transactions on Neural Networks*, vol. 19, no. 1, pp. 18–39, 2008.
- [29] M. Blondel, M. Ishihata, A. Fujino, and N. Ueda, “Polynomial networks and factorization machines: new insights and efficient training algorithms,” in *Proc. ICML*, Jun. 2016, pp. 850–858.

- [30] Z.-Y. Han, J. Wang, H. Fan, L. Wang, and P. Zhang, “Unsupervised generative modeling using matrix product states,” *Physical Review X*, vol. 8, no. 3, p. 031012, 2018.
- [31] D. Liu, S.-J. Ran, P. Wittek, C. Peng, R. B. García, G. Su, and M. Lewenstein, “Machine learning by two-dimensional hierarchical tensor networks: A quantum information theoretic perspective on deep architectures,” in *Proc. ICLR*, May 2018.
- [32] I. Glasser, N. Pancotti, and J. I. Cirac. (2018) Supervised learning with generalized tensor networks. [Online]. Available: <https://arxiv.org/abs/1806.05964>
- [33] D. T. Tran, M. Yamaç, A. Degerli, M. Gabbouj, and A. Iosifidis, “Multilinear compressive learning,” *IEEE Transactions on Neural Networks and Learning Systems*, pp. 1–13, 2020.
- [34] S. Efthymiou, J. Hidary, and S. Leichenauer. (2019) TensorNetwork for machine learning. [Online]. Available: <https://arxiv.org/abs/1906.06329>
- [35] K. He, X. Zhang, S. Ren, and J. Sun, “Identity mappings in deep residual networks,” in *Proc. ECCV*, Oct. 2016, pp. 630–645.
- [36] A. Veit, M. J. Wilber, and S. Belongie, “Residual networks behave like ensembles of relatively shallow networks,” in *Advances in Neural Information Processing Systems*, D. Lee, M. Sugiyama, U. Luxburg, I. Guyon, and R. Garnett, Eds., vol. 29, 2016.
- [37] Y. LeCun, B. Boser, J. S. Denker, D. Henderson, R. E. Howard, W. Hubbard, and L. D. Jackel, “Backpropagation applied to handwritten zip code recognition,” *Neural Computation*, vol. 1, no. 4, pp. 541–551, 1989.
- [38] S. S. Schoenholz, J. Gilmer, S. Ganguli, and J. Sohl-Dickstein, “Deep information propagation,” in *Proc. ICLR*, Apr. 2017.
- [39] V. Vapnik, *The Nature of Statistical Learning Theory*. Springer science & business media, 2013.
- [40] D. P. Kingma and J. Ba, “Adam: A method for stochastic optimization,” *arXiv preprint arXiv:1412.6980*, 2014.
- [41] A. Paszke, S. Gross, F. Massa, A. Lerer, J. Bradbury, G. Chanan, T. Killeen, Z. Lin, N. Gimelshein, L. Antiga *et al.*, “Pytorch: An imperative style, high-performance deep learning library,” in *Proc. NIPS*, Dec. 2019, pp. 8026–8037.
- [42] S. Ioffe and C. Szegedy, “Batch normalization: Accelerating deep network training by reducing internal covariate shift,” in *Proc. ICML*, Jul. 2015, pp. 448–456.
- [43] A. Krizhevsky, I. Sutskever, and G. E. Hinton, “Imagenet classification with deep convolutional neural networks,” *Communications of the ACM*, vol. 60, no. 6, pp. 84–90, 2017.